Available online at www.sciencedirect.com
ScienceDirect
Journal of Controlled Release 115 (2006) 18–25
journal of controlled release
www.elsevier.com/locate/jconrel

Slow release of molecules in self-assembling peptide nanofiber scaffold

Yusuke Nagai [a,b], Larry D. Unsworth [a,c], Sotirios Koutsopoulos [a], Shuguang Zhang [a,*]

[a] Center for Biomedical Engineering, Massachusetts Institute of Technology, 77 Massachusetts Avenue, Cambridge, Cambridge, MA 02139-4307, USA
[b] Menicon Co., Ltd. 5-1-10 Takamoridai, Kasugai, Aichi 487-0032, Japan
[c] National Research Council — National Institute for Nanotechnology, 9107-116 Street/University of Alberta, Edmonton, Alberta, Canada T6G 2V4

Received 12 May 2006; accepted 30 June 2006
Available online 8 July 2006

Abstract

Biological hydrogels consisting of self-assembling peptide nanofibers are potentially excellent materials for various controlled molecular release applications. The individual nanofiber consists of ionic self-complementary peptides with 16 amino acids (RADA16, Ac-RADARADARADARADA-$CONH_2$) that are characterized by a stable β-sheet structure and undergo self-assembly into hydrogels containing ~99.5% w/v water. We report here on the diffusion properties of phenol red, bromophenol blue, 8-hydroxypyrene-1,3,6-trisulfonic acid trisodium salt (pyranine, 3-PSA), 1,3,6,8-pyrenetetrasulfonic acid tetrasodium salt (4-PSA), and Coomassie Brilliant Blue G-250 (CBBG) through RADA16 hydrogels. The apparent diffusivity ($\bar{D}$) of phenol red ($1.05\pm0.08\times10^{-10}$ m^2 s^{-1}) is higher than that of 3-PSA ($0.050\pm0.004\times10^{-10}$ m^2 s^{-1}) and 4-PSA ($0.007\pm0.002\times10^{-10}$ m^2 s^{-1}). The difference in 3-PSA and 4-PSA diffusivities suggests that the sulfonic acid groups directly facilitate electrostatic interactions with the RADA16 fiber surface. Bromophenol blue and CBBG were not released from the hydrogel, suggesting that they interact strongly with the peptide hydrogel scaffold. The diffusivities ($\bar{D}$) of the dyes decreased with increasing hydrogel peptide concentration, providing an alternate route of controlling release kinetics. These results indicate that release profiles can be tailored through controlling nanofiber-diffusant molecular level interactions.

Keywords: Self-assembling peptides; Nanofiber scaffold hydrogel; Diffusion coefficient; Controlled molecule release

1. Introduction

Self-assembling peptide nanofiber based hydrogels can be used in a broad range of biomedical and biotechnological applications ranging from 3D scaffolds for tissue engineering to drug delivery vehicles [1–3]. Short peptides (8–16 residues or 2.5–5 nm in length) are chemically synthesized and form β-sheet structures in water [4–7]. Depending on the pH and the ionic strength of the medium these peptides self-assemble into nanofibers, which in turn form a hydrogel. These hydrogel systems are well characterized and have already been employed in a variety of 3D tissue cell cultures and tissue engineering research applications [8–14].

A significant increase in therapeutic efficacy can be realized through incorporating controlled release strategies into the design of drug delivery systems [15–19]. Developing a drug release system that is not only efficient, biocompatible, robust, but also useful for diverse applications requires a material that can deliver active compounds, at specific rates, throughout the entire therapy regimen. Thus, controlling the release rates of small molecules and peptides/proteins through various hydrogels is crucial. Self-assembling peptide hydrogels are an important class of hydrogels, which are potentially good candidates for providing a robust drug delivery system. When compared to chemically synthesized polymer materials, self-assembling peptide nanofiber hydrogels are generally more biocompatible [1,2], able to respond to external stimuli under various physiological conditions and maintain a high water content (i.e., ca. 99.5% w/v): the latter may allow for the diffusion of a wide range of molecules. Furthermore, self-assembling peptide nanofiber hydrogels are amenable to molecular design and can be tailored for the specific needs of the application.

* Corresponding author. Center for Biomedical Engineering, Massachusetts Institute of Technology, NE47-Room 379, 500 Technology Square, Cambridge, MA 02139-4307, USA. Tel.: +1 617 258 7514; fax: +1 617 258 5239.
E-mail address: shuguang@mit.edu (S. Zhang).

0168-3659/$ - see front matter © 2006 Elsevier B.V. All rights reserved.
doi:10.1016/j.jconrel.2006.06.031

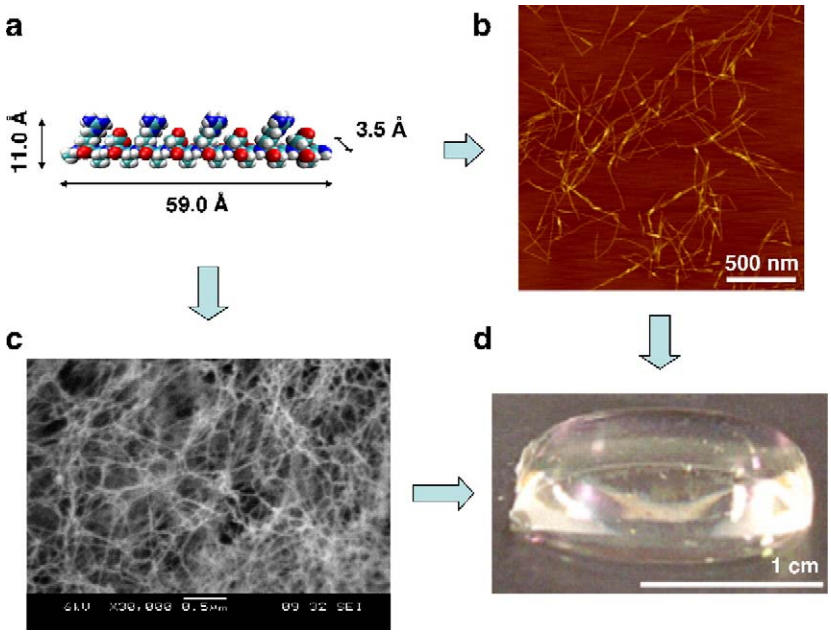

Fig. 1. The self-assembling peptide scaffold. (a) Molecular model of RADA16, the dimensions of which are 59.0 Å × 11.0 Å × 3.5 Å. For the representation the VMD software was used: cyan, carbons; red, oxygen; blue, nitrogen; white, hydrogen. (b) AFM image of the RADA16 nanofibers. (c) SEM image of the RADA16 hydrogel. (d) Image of the RADA16 hydrogel with high water content, i.e., >99.5% w/v (photograph by Dr. Hidenori Yokoi).

Herein, we investigated the effect of the model drug properties (charge and structure) on their release kinetics through self-assembling peptide hydrogels (Fig. 1). Phenol red, bromophenol blue, 8-hydroxypyrene-1,3,6-trisulfonic acid trisodium salt (3-PSA), 1,3,6,8-pyrenetetrasulfonic acid tetrasodium salt (4-PSA), and Coomassie Brilliant Blue G-250 (CBBG) were chosen as model drugs for several reasons: (1) they are well characterized dyes that have been used to investigate drug interactions with the liver (phenol red and bromophenol blue) [20,21] and as anionic probes for sensor applications (3-PSA and 4-PSA) [22,23]; (2) these molecules should allow for the systematic investigation of charge effects on drug diffusion through peptide hydrogels due to both their physical properties and the specific amounts of sulfonic acid and amine groups present (Fig. 2). The release kinetics of compounds dispersed throughout a hydrogel are predominantly controlled by diffusion [24]. The diffusion coefficients of these model compounds through our hydrogel will be calculated using standard methodologies [25–27]. Furthermore, by correlating the model drug properties to the resulting diffusion coefficients it is possible to discuss the release mechanism.

2. Experimental

2.1. Materials

The self-assembling peptide RADA16 (Ac-RADARADAR-ADARADA-$CONH_2$, PuraMatrix™) 3% (w/v in PBS, pH=3) was obtained from 3DM Inc. (Cambridge, MA, USA). Phenol red (MW=354.4), bromophenol blue sodium salt (MW=691.9), 8-hydroxypyrene-1,3,6-trisulfonic acid trisodium salt (3-PSA, pyranine, MW=524.4), 1,3,6,8-pyrenetetrasulfonic acid tetrasodium salt (4-PSA, MW=610.4) and Coomassie Brilliant Blue G-250 (CBBG, MW=854.0) were purchased from Sigma-Aldrich and dissolved in Milli-Q water to prepare 0.8 and 1.06 mM solutions.

2.2. Diffusion experiments of dyes through the peptide gel

RADA16 was diluted with Milli-Q water to 1.5% w/v and mixed with the dye solution (0.8 mM) at a ratio of 1:2. The final

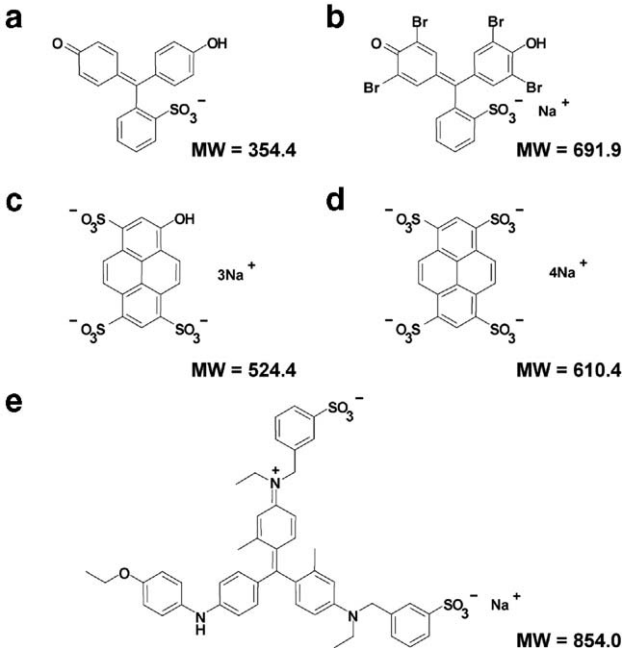

Fig. 2. Molecular structure of the dye molecules: (a) phenol red, (b) bromophenol blue, (c) 8-hydroxypyrene-1,3,6-trisulfonic acid trisodium salt (3-PSA), (d) 1,3,6,8-pyrenetetrasulfonic acid tetrasodium salt (4-PSA) and (e) Coomassie Brilliant Blue G-250 (CBBG).

concentrations of the RADA16 and the dye in the mixture were 0.5% w/v (2.9 mM) and 0.53 mM, respectively. 100 μl of the mixture was placed at the bottom of 1 ml tubes (SepCap Vials, 6.4 mm × 40 mm) and the hydrogel formed overnight at room temperature. Then, 900 μl of isotonic saline solution (0.9% w/v NaCl) was slowly added to each tube so as to not disrupt the hydrogel structure. The release experiments were performed at 37 °C, for a period of 7 days, where the supernatant dye concentration was measured at 15 min, 30 min, 1, 2, 4, 8 h, after which we sampled every 8 h. The concentration of the dye molecules in the supernatant was measured by a NanoDrop Spectrophotometer (ND-1000 UV–Vis, NanoDrop Technologies, Delaware, USA) using 1.5 μl aliquots. The concentration of the dye released from the hydrogel was determined using a calibration curve of the pure dye in isotonic saline solution at the wavelength where they showed their maximum absorbance, i.e., phenol red at 429 nm, bromophenol blue at 592 nm, 3-PSA at 404 nm, 4-PSA at 373 nm, and CBBG at 583 nm. To examine the effect peptide density has on drug release kinetics hydrogels were formed using the same procedure as above, with RADA16 concentrations of 1 and 1.5%.

2.3. Scanning electron microscopy (SEM) and atomic force microscopy (AFM) analyses

Prior to SEM analysis, peptide hydrogels were dehydrated using a Tousimis Sam-Dri 1000 critical point dryer, coated with an Au–Pd layer and examined using a Jeol JSM 6060 SEM: 6 kV acceleration voltage and 12 mm electronic working distance.

AFM images were recorded using a Nanoscope IIIa (Digital Instruments, Santa Barbara, CA) operated in tapping mode at a frequency of 60 kHz. After sonication for 30 min, a small portion of the RADA16 hydrogel was diluted 20 times in Milli-Q water and 1 μl of the final solution was deposited on a freshly cleaved mica surface and was allowed to dry. Soft silicon cantilevers of 219 μm length were used (Veeco Probes) with spring constant 1–5 N/m and tip radius of curvature 5–10 nm. AFM images were taken at 512 × 512 pixels resolution. The root mean square (RMS) amplitude before tip–surface contact was 1.0–1.2 V, the integral and proportional gains were 0.2–0.6 and 0.4–1.2, and the set point and scanning speed were 0.7–1.0 V and 1.0–1.5 Hz, respectively.

2.4. Molecular modeling

The molecular models of RADA16 anti-parallel β-sheet structure and the resulting fiber were produced using Facio, a 3D-graphics program, employing Tinker with a charrm19 force field parameter (http://www1.bbiq.jp/zzzfelis/Facio.html and http://dasher.wustl.edu/tinker/) [28,29]. In order to model the fiber structure the distance between RADA16 along the fiber backbone was assumed to be 4.8 Å and the inter-sheet distance was set to 1.0 nm, as defined by the gap between two planes spanned by C-alpha carbons belonging to each layer. The graphic illustration of the result was generated using VMD software (http://www.ks.uiuc.edu/Research/vmd/) [30].

3. Theory

Release experiments, utilizing thin hydrogel films containing molecularly dispersed 'drug', provide a route for calculating the hydrogel-specific apparent diffusion coefficients. Assuming an adequate diffusion sink, with a significantly larger volume and a significantly greater drug diffusion coefficient than that of the hydrogel, we can ignore the transport within the sink when calculating the overall release rate of the drug from the hydrogel (Fig. 3). Given these conditions, the 1D unsteady-state form of Fick's second law of diffusion for a plane film of thickness, H, is:

$$\frac{\delta c}{\delta t} = D\frac{\delta^2 c}{\delta x^2} \tag{1}$$

where D is the diffusion coefficient of the active agent in the hydrogel and c is the concentration of the drug as a function of time (t) and position (x) [31–33]. Given that diffusion is concentration independent and only occurs in the positive x direction, from the hydrogel to the sink, and assuming that (1) the rate at which the substance is transported to the surface is equal to the internal diffusion rate, (2) absence of solute–carrier interactions and (3) at time zero the hydrogel surface is quickly brought into contact with the perfect sink, then Eq. (1) can be transformed to [31]:

$$\frac{M_t}{M_\infty} = 4\left(\frac{Dt}{H^2}\right)^{0.5}\left[\frac{1}{\pi^{0.5}} + 2\sum_{n=0}^{\infty}(-1)^n i\mathrm{erfc}\frac{n\ H}{2(Dt)^{0.5}}\right] \tag{2}$$

where M_t and M_∞ are the total mass of the diffusing compounds released from the layer after time t and infinite time, respectively. For small values of t, Eq. (2) can be reduced to:

$$\frac{M_t}{M_\infty} = \left(\frac{16\ Dt}{\pi\ H^2}\right)^{0.5} \tag{3}$$

where the diffusion coefficient is constant. However, for most systems, the diffusion coefficient is dependent on drug

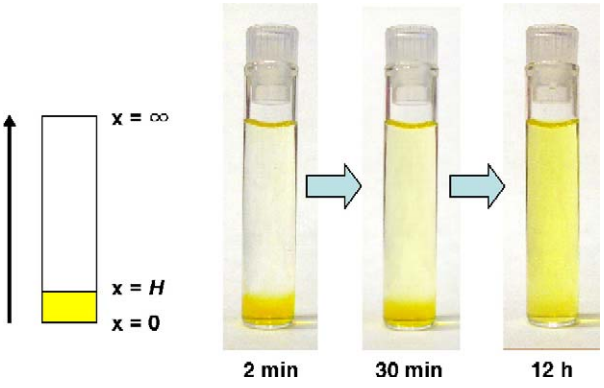

Fig. 3. Definition sketch and experimental conditions used to study diffusion of compounds from the hydrogel (sky blue). The pictures were taken during a typical experiment using 0.5% w/v RADA16 peptide hydrogel and phenol red as a diffusing molecule 2, 30 min and 12 h. The color intensity of the bulk solution increased with time as a result of phenol red release (for interpretation of the references to color in this figure legend, the reader is referred to the web version of this article).

concentration as well as the concentration of the swelling agent (i.e., water). In these cases, the slope (θ_1) of M_t/M_∞ as a function of $t^{0.5}$ yields an average diffusion coefficient ($\bar{D}$). It should be mentioned that due to the fact there exists an interaction between the solute and the nanofibers the calculated diffusivities are considered to be apparent diffusivities and allow for a comparison of the systems under study.

Eq. (2) can also be recast into the following form:

$$\frac{M_t}{M_\infty} = 1 - \frac{8}{\pi^2}\sum_{m=0}^{\infty}\frac{1}{(2m+1)^2}\exp\left[-\frac{D(2m+1)^2\pi^2 t}{H^2}\right] \quad (4)$$

As the drug concentration approaches zero, *viz*., after a long diffusion time, all exponential terms can be neglected except the first one, yielding:

$$\ln(M_{\infty - M_t}) = \ln\left(\frac{8M_\infty}{\pi^2}\right) - \theta_2 t \quad (5)$$

$$\theta_2 = -\frac{D_0\pi^2}{H^2} \quad (6)$$

where D_0 is the diffusion coefficient as the drug concentration within the hydrogel approaches zero. Using these relationships, the steady-state permeation rate (J) of the drug can be calculated using:

$$J = \frac{D_0}{\beta H}\left[e^{\beta c_\infty} - 1\right] \quad (7)$$

$$\bar{D} = \frac{D_0}{c_\infty \beta}\left[e^{\beta c_\infty} - 1\right] \quad (8)$$

where β is a system dependant constant.

The Stokes–Einstein equation (Eq. (9)) calculates the free bulk diffusion coefficient as a function of the Boltzmann constant (k_B), temperature (T), solvent dynamic viscosity (μ) and solute radius (r_H).

$$D_{S-E} = \frac{k_B T}{6\pi\ \mu\ r_H} \quad (9)$$

The various parameters were determined using the following regimen:

1. $\bar{D}$ was solved from the slope (θ_1) of $0 < M_t/M_\infty < 0.6$ versus $t^{0.5}$: for short times.
2. D_0 was determined from θ_2: for long times.
3. β was determined using the Excel 'Solver' routine, where β was varied such that Eq. (8) was resolved. Solver parameters were set to the following constraints: iterations = 1000; precision = 1×10^{-15}; tolerance = 2%; convergence = 1×10^{-17} and all values converged to values of 1×10^{-16}.
4. J was calculated using Eq. (7).
5. D_{S-E} was calculated using Eq. (9).

4. Result and discussion

In order to interpret the results obtained for the diffusion of these dyes through the self-assembling peptide nanofiber hydrogel, it is imperative that the physicochemical characteristics of the peptide hydrogel and the structural, and the chemical, properties of the dye molecules are taken into consideration. RADA16 nanofibers have a hydrophilic surface composed of alternating arginine (positive charge) and aspartic acid (negative charge) residues [1,34] that intertwine to form a hydrogel (Fig. 1) with a large surface to volume ratio. The pH of the system was held at pH ~3. At this pH sulfonic acid groups (Fig. 2) of the dye molecules are deprotonated [35–39]. Whereas the hydroxyl groups of 3-PSA (pK_a = 7.3), phenol

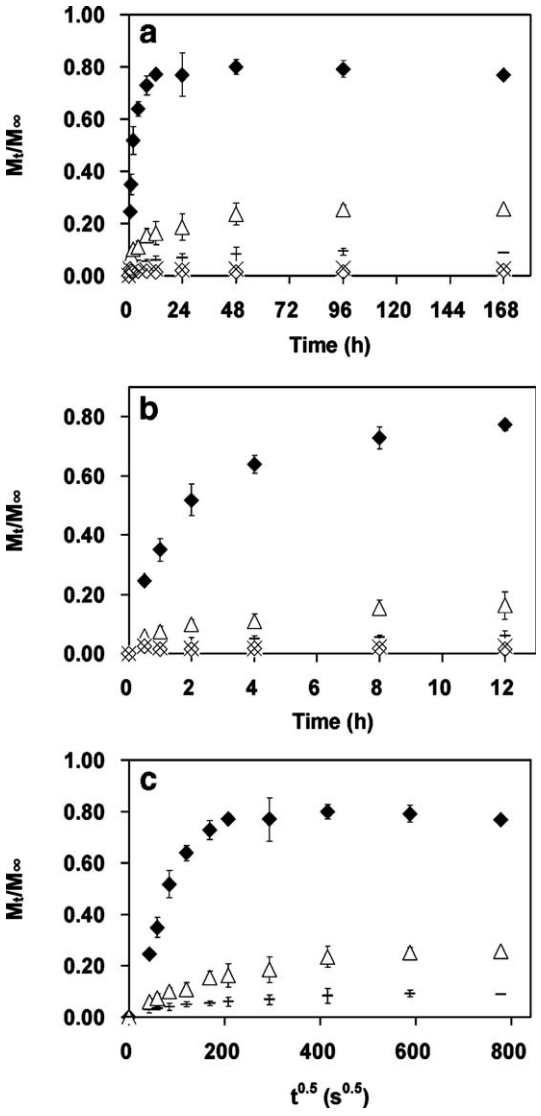

Fig. 4. Measured release kinetics of dye molecules through the hydrogel: (◆) phenol red, (×) bromophenol blue, (△) 3-PSA, (—) 4-PSA and (◇) CBBG. (a) Cumulative dye release as a function of time. The plots show three types of diffusion kinetics through the hydrogel: fast diffusion (i.e., phenol red), slow diffusion (i.e., 3-PSA and 4-PSA) and no diffusion (i.e., bromophenol blue and CBBG). (b) Cumulative dye release results for first 12 h. (c) Plots of M_t/M_∞ as a function of $t^{0.5}$ for the dyes released from the hydrogel, (i.e., phenol red, 3-PSA, and 4-PSA). Data points are average of n = 3 and error bars represent ±1 SD.

Table 1
Diffusion parameters and calculated values for the compounds released from RADA16 hydrogels

	Phenol red	3-PSA	4-PSA
$V\times10^{-3}$ (l)*	0.84±0.01	0.84±0.01	0.84±0.01
$H\times10^{-3}$ (m)*	4.2±0.5	4.2±0.5	4.2±0.5
$r\times10^{-10}$ (m)	6.2	5.8	5.8
$r_H\times10^{-10}$ (m)	8.5	8.1	8.1
$\theta_1\times10^{-3}$**	5.6±0.2	1.23±0.05	0.46±0.05
R^2_1	0.97	0.93	0.24
$\theta_2\times10^{-5}$**	−2.0±0.3	−0.069±0.002	−0.005±0.001
R^2_2	0.98	0.99	0.99
$\bar{D}\times10^{-10}$ ($m^2\ s^{-1}$)***	1.05±0.08	0.050±0.004	0.007±0.002
$D_0\times10^{-10}$ ($m^2\ s^{-1}$)***	0.34±0.06	0.012±0.001	0.0008±0.0002
$D_{S-E}\times10^{-10}$ ($m^2\ s^{-1}$)	2.84	2.98	2.98
β	0.087	0.045	0.078
$J\times10^{-6}$ ($\mu g\ m^{-2}\ s^{-1}$)***	5.7±0.7	0.66±0.02	0.08±0.01

* Errors determined from standard deviation calculation where $n=3$.
** Errors in slope determined using 'linest': Excel function for determining error in slopes.
*** Errors determined using standard error propagation techniques.

red ($pK_a=7.9$) are strongly protonated, while bromophenol blue ($pK_a=4$) is only weakly protonated.

4.1. Release profile of the dyes from 0.5% w/v peptide hydrogel

The mass-transfer kinetics for the release of the dyes from the 0.5% w/v peptide nanofiber hydrogel are illustrated in Fig. 4a, as a plot of mass released fraction (M_t/M_∞) as a function of time (t). Based on the release kinetics of the diffusing compounds we were able to categorize the dyes into three groups: fast released dye (phenol red), slow released dyes (3-PSA and 4-PSA), and non-released dyes (bromophenol blue and CBBG). A summary of the data analysis for the dyes released from the 0.5% w/v peptide hydrogel are presented in Table 1. Such an analysis could not be performed for bromophenol blue and CBBG, since they were essentially retained in the peptide scaffold even after 7 days. As illustrated in Fig. 4b, the M_t/M_∞ ratio as a function of $t^{0.5}$ for the dyes that were released from the peptide hydrogel was non-linear, suggesting that the diffusion behavior of these systems was non-Fickian in nature.

The concentration of phenol red in the supernatant increased quickly, more than 50% of the loaded amount was released from the peptide scaffold after 2 h and reached a plateau after 12 h. Calculated diffusivity and permeation rate for phenol red were $1.05\pm0.08\times10^{-10}$ $m^2\ s^{-1}$ and $5.7\pm0.7\times10^{-6}$ $\mu g\cdot m^{-2}\ s^{-1}$, respectively. The Stokes–Einstein diffusivity (D_{S-E} Eq. (9)) for phenol red, in aqueous solution, was 2.84×10^{-10} $m^2\ s^{-1}$, about five times smaller than the experimentally determined diffusivity. This difference is most likely due to the presence of the nanofiber and its interaction with the diffusant.

Although phenol red and bromophenol blue have similar molecular structures, the former was readily released from the hydrogel while the latter was not. This may be explained in terms of the acidic properties of the dyes. Bromophenol blue has a lower pK_a value than phenol red. This is due to the presence of electron-attracting groups of the bromophenol blue phenol rings, which in turn retain fewer electrons in the ring as compared to the aromatic rings of phenol red [35]. Hence, the phenolic hydroxyl group of bromophenol blue is a stronger acid than the one in phenol red. Thus, the hydroxyl group of bromophenol blue tends to be dissociated in the hydrogel microenvironment (ca. pH=3), which could facilitate a stronger electrostatic interaction between bromophenol blue and the peptide nanofibers as compared to those between phenol red and the nanofibers.

It was anticipated that the interaction of the acidic hydrogel (pH ~3) with bromophenol blue, which is commonly used as a pH indicator, would result in changing the color of the dye. This was indeed the case with phenol red ($pK=7.9$), which upon mixing with the hydrogel changed its color from red to yellow. Because bromophenol blue has a pK value of 4.0, a similar color change was expected upon mixing with the hydrogel. However, we did not observe such a color change and bromophenol blue remained blue throughout the course of the measurements.

This phenomenon has been previously investigated when the interaction of bromophenol blue with bovine serum albumin (BSA) was studied [40,41]. Even under acidic conditions, the mixing of bromophenol blue and BSA did not lead to a change in the color of the solution but resulted in a stable blue complex with a bathochromic shift of the bromophenol blue absorption spectra. This was attributed to the electrostatic interactions between positively charged amines and phenolic hydroxyl groups of bromophenol blue, whose acidic properties were enhanced by the presence of electron-attracting groups. This property of bromophenol blue led to the development of a methodology for determining solution protein concentration [42,43]. Hence, it is possible that bromophenol blue interacts strongly with the RADA16 peptide nanofibers, in a similar manner, *viz*., electrostatic interactions between the phenolic hydroxyl group of bromophenol blue and the positively charged amines of the arginine residues of the self-assembling peptide hydrogel.

The mass fraction of the released 3-PSA and 4-PSA reached 26% and 9% after 7 days, respectively. Compared to phenol red ($1.05\pm0.08\times10^{-10}$ $m^2\ s^{-1}$), 3-PSA and 4-PSA were slowly released from the hydrogel, yielding respective apparent diffusivities and permeation rates of: 0.050 ± 0.004 and $0.007\pm0.002\times10^{-10}$ $m^2\ s^{-1}$; 0.66 ± 0.02 and $0.08\pm0.01\times10^{-6}$ $\mu g\ m^{-2}\ s^{-1}$. Furthermore, when compared to the theoretical diffusivities (D_{S-E}) of 2.98×10^{-10} $m^2\ s^{-1}$ for both 3-PSA and 4-PSA in water, the respective experimentally determined diffusivities of 0.050 ± 0.004 and $0.0071\pm0.0015\times10^{-10}$ $m^2\ s^{-1}$ for 3-PSA and 4-PSA were considerably smaller. This may indicate that the peptide fibers interact with 3-PSA and 4-PSA in the hydrogel matrix. Additionally, a comparison of the initial release kinetics shows that the diffusivity of 3-PSA is about seven times higher than that of 4-PSA. These two molecules have similar size and structural characteristics and differ only in one sulfonic acid group: 4-PSA has 4 sulfonic side groups while 3-PSA has 3 sulfonic groups and one hydroxyl group (Fig. 2). It is supposed that the difference in the release rates is probably due to electrostatic interactions between the sulfonic acid groups and the positively charged amine groups of the peptide nanofibers [22,23].

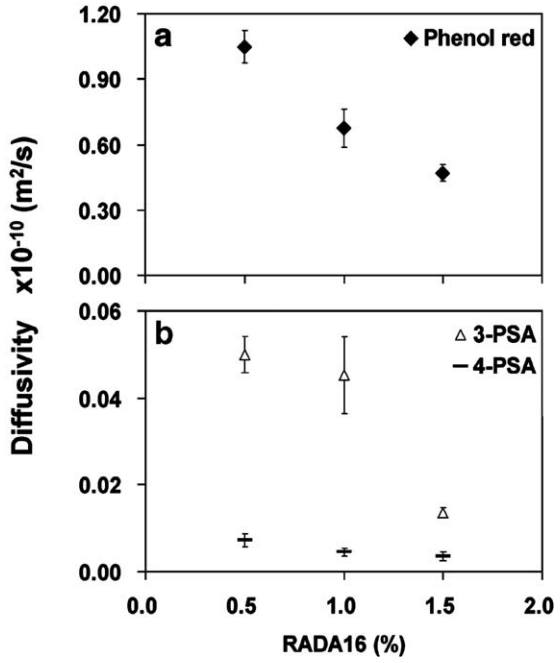

Fig. 5. Calculated diffusivities of phenol red (♦), 3-PSA (Δ) and 4-PSA (—) from 0.5%, 1% and 1.5% w/v peptide hydrogels. In all cases we observed a decrease of the average values of the diffusivities with increasing peptide concentration. Data points are average of $n=3$ and error bars represent ±1 SD.

Although CBBG is a significantly larger molecule than the others used in this study its release kinetics were interpreted using the same arguments evoked for bromophenol blue. If we compare the release profiles from Fig. 4 we see that: 1. phenol red, PSA and bromophenol blue are similar sizes with significantly different release rates; 2. CBBG and bromophenol blue were very different in size and neither were released from the gel. Therefore, it was concluded that for these systems solute size did not dictate their release profiles. As CBBG binds strongly to proteins, for which it is used in the Bradford assay to determine protein concentration, it is concluded that this interaction inhibits its release from the peptide based hydrogel [44]. The strong binding of CBBG to proteins was attributed to the ionized sulfonic groups of the dye that strongly interact with the amino acids' charged side groups [45].

4.2. Effect of the peptide density in the hydrogel

The respective apparent diffusivities of phenol red, 3-PSA and 4-PSA were: 0.67±0.09, 0.045±0.009 and 0.0044±0.0009×10^{-10} m^2 s^{-1} in 1% w/v; 0.47±0.04, 0.014±0.001 and 0.0035±0.0011×10^{-10} m^2 s^{-1} in 1.5% w/v peptide hydrogel, respectively. The diffusivities are plotted as a function of the peptide concentration in Fig. 5, where average diffusivities show similar trends in that the higher the peptide concentration the lower the diffusivity. This result suggests that the drug release profile from these hydrogels can be controlled by changing the peptide concentration of the hydrogel.

In a previous work the release of methoxytryptamine was studied using β-cyclodextrin and hydroxyethyl acrylate hydrogels [46]. It was observed that the release kinetics were directly related to the concentration of β-cyclodextrin, where higher β-cyclodextrin concentrations resulted in slower drug release rates. β-cyclodextrin and methoxytryptamine form inclusion complexes with 1:1 ratios [46]. Therefore, the concentration of β-cyclodextrin was interpreted to be the dominant factor in controlling drug release from the hydrogel. In our study, the peptide nanofiber surface also interacts with the diffusant. Likewise, as the peptide concentration increases (along with the nanofiber surface area), it is supposed that the probability of nanofiber-diffusant interactions also increases, yielding a decrease in apparent diffusivity. Therefore, the apparent diffusivities of anionic compounds can be controlled by changing the peptide fiber concentration.

4.3. Proposed interaction mechanism between model 'drugs' and peptide nanofibers

In order to further understand the possible role of the sulfonic acid groups on the release kinetics of 3- and 4-PSA a molecular model of the interaction between RADA16 nanofibers and 4-PSA was constructed (Fig. 6). The distance between neighboring amines of the arginines in RADA16 is approximately 11.8 Å. This is comparable with the calculated average distances between the oxygens of the sulfonic acids of 3- and 4-PSA (6.7, 8.1 and 10.4 Å). Hence, it is structurally possible for 3- and 4-PSA to form multiple contact points with the RADA16 nanofibers. In

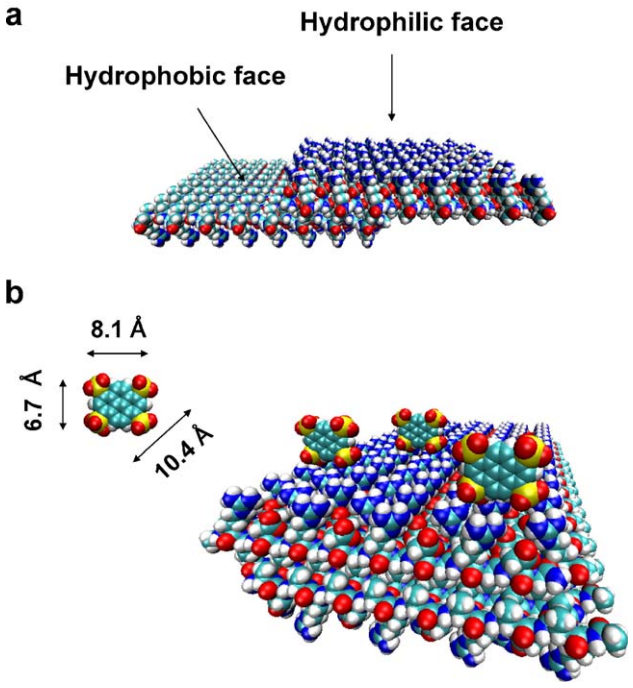

Fig. 6. Illustration of the molecular modeling results for self-assembling RADA16 peptide nanofibers: (a) hydrophobic alanine side groups are present on one side of the RADA16 β-sheet and the other side is populated with alternating positive and negative charges due to the arginine and aspartic acid residues, respectively. (b) Illustration of the interaction between 4-PSA and RADA16 nanofiber shows that the interatomic distances between the sulfonic acid groups of 4-PSA line up with the arginines on the peptide nanofiber, where: cyan, carbons; red, oxygen; blue, nitrogen; white, hydrogen; yellow, sulfur (for interpretation of the references to color in this figure legend, the reader is referred to the web version of this article).

RADA16 nanofibers the non-polar alanine residues reside in the interior and the polar residues (arginines with pK_a=11.5–12.5 and aspartic acid with pK_a=3.0–5.5) are on the surface [1]. The aspartic acid residues are shorter than the arginines. Therefore, in the β-sheet conformation the longer positively charged arginine side groups stand out of the nanofiber. It is supposed that the absence of one sulfonic group allows 3-PSA to be released faster than 4-PSA from the peptide nanofiber hydrogel.

Our findings are in line with previous investigations, which showed that multiple-point interactions facilitated the capture of 3- and 4-PSA by methacrylamidopropyltrimethylammonium chloride (MAPTAC, positive charge) that was present in a shrinkable gel composed of *N*-isopropylacrylamide (NIPA) and *N*,*N* 9-methylenebisacrylamide (BIS) [38]. In our case, the abundance of positively charged amines on the nanofiber allows for multiple-point interactions with 3- and 4-PSA and the nanofiber-4-PSA interaction is stronger due to the presence of an additional sulfonic acid group.

5. Conclusions

As controlled drug release enters into more and more applications in medicine there is a growing interest in developing a system that is amenable to molecular design and can be tailor-made for the specific drugs. We studied the possibility of using a hydrogel consisting of self-assembling peptides as a carrier for controlled drug release. The diffusing molecules were chosen so as to model the diffusion of drug compounds that have similar sizes and molecular structures, but varying charge densities. Our data shows that the release kinetics of the dyes studied depended on their structure, the number of available charged groups and the peptide concentration in the hydrogel. The small differences observed in the release kinetics between 3-PSA and 4-PSA may suggest that their diffusion rates can be controlled by adjusting the amino acid sequence of the engineered peptides. The same principle may be applied in the case of bromophenol blue and CBBG that were retained in the hydrogel because of their property to bind strongly to the peptide nanofibers. As before, the tailor-made properties of the peptide nanofibers could provide a sufficient number and specific types of charged amino acids to control the release rates of drugs through the hydrogel.

Acknowledgement

We thank Dr. Jiyong Park and Dr. Wonmuk Hwang for kindly sharing with us their unpublished results and stimulating discussions on the molecular modeling of the RADA16 peptide and to Aki Nagai for helpful discussions on the experimental details. Y.N. gratefully acknowledges the generous support from Menicon Ltd. Japan and S.K. was supported by the HighQ Foundation.

References

[1] S. Zhang, Fabrication of novel biomaterials through molecular self-assembly, Nat. Biotechnol. 21 (2003) 1171–1178.
[2] S. Zhang, Emerging biological materials through molecular self-assembly, Biotechnol. Adv. 20 (2002) 321–339.
[3] C. Keyes-Baig, J. Duhamel, S.Y. Fung, J. Bezaire, P. Chen, Self-assembling peptide as a potential carrier of hydrophobic compounds, J. Am. Chem. Soc. 126 (2004) 7522–7532.
[4] S. Zhang, T. Holmes, C. Lockshin, A. Rich, Spontaneous assembly of a self-complementary oligopeptide to form a stable macroscopic membrane, Proc. Natl. Acad. Sci. U. S. A. 90 (1993) 3334–3338.
[5] S. Zhang, C. Lockshin, R. Cook, A. Rich, Unusually stable β-sheet formation in an ionic self-complementary oligopeptide, Biopolymers 34 (1994) 663–672.
[6] S. Zhang, T. Holmes, M. DiPersio, R.O. Hynes, X. Su, A. Rich, Self-complementary oligopeptide matrices support mammalian cell attachment, Biomaterials 16 (1995) 1385–1393.
[7] H. Yokoi, T. Kinoshita, S. Zhang, Dynamic reassembly of peptide RADA16 nanofiber scaffold, Proc. Natl. Acad. Sci. U. S. A. 102 (2005) 8414–8419.
[8] T. Holmes, S. Delacalle, X. Su, A. Rich, S. Zhang, Extensive neurite outgrowth and active neuronal synapses on peptide scaffolds, Proc. Natl. Acad. Sci. U. S. A. 97 (2000) 6728–6733.
[9] J. Kisiday, M. Jin, B. Kurz, H. Hung, C.E. Semino, S. Zhang, A.J. Grodzinsky, Self-assembling peptide hydrogel fosters chondrocyte extracellular matrix production and cell division: implications for cartilage tissue repair, Proc. Natl. Acad. Sci. U. S. A. 99 (2002) 9996–10001.
[10] S. Zhang, F. Gelain, X. Zhao, Designer self-assembling peptide nanofiber scaffolds for 3D tissue cell cultures, Semin. Cancer Biol. 15 (2005) 413–420.
[11] M.E. Davis, J.P.M. Motion, D.A. Narmoneva, T. Takahashi, D. Hakuno, R.D. Kamm, S. Zhang, R.T. Lee, Injectable self-assembling peptide nanofibers create intramyocardial microenvironments for endothelial cells, Circulation 111 (2005) 442–450.
[12] D.A. Narmoneva, O. Oni, A.L. Sieminski, S. Zhang, J.P. Gertler, R.D. Kamm, R.T. Lee, Self-assembling short oligopeptides and the promotion of angiogenesis, Biomaterials 26 (2005) 4837–4846.
[13] M.A. Bokhari, G. Akay, S. Zhang, M.A. Birch, The enhancement of osteoblast growth and differentiation in vitro on a peptide hydrogel–polyHIPE polymer hybrid material, Biomaterials 26 (2005) 5198–5208.
[14] R. Ellis-Behnke, Y.X. Liang, S.W. You, D. Tay, S. Zhang, K.F. So, G. Schneider, Nano neuro knitting: peptide nanofiber scaffold for brain repair and axon regeneration with functional return of vision, Proc. Natl. Acad. Sci. U. S. A. 103 (2006) 5054–5059.
[15] M. Hombreiro-Perez, J. Siepmann, C. Zinutti, A. Lamprecht, N. Ubrich, M. Hoffman, R. Bodmeier, P. Maincent, Non-degradable microparticles containing a hydrophilic and/or a lipophilic drug: preparation, characterization and drug release modeling, J. Control. Release 88 (2003) 413–428.
[16] L.W. Wang, S. Venkatraman, L. Kleiner, Drug release from injectable depots: two different in vitro mechanisms, J. Control. Release 99 (2004) 207–216.
[17] P. Gupta, K. Vermani, S. Garg, Hydrogels: from controlled release to pH-responsive drug delivery, Drug Discov. Today 7 (2002) 569–579.
[18] H.Y. He, X. Cao, L.J. Lee, Design of a novel hydrogel-based intelligent system for controlled drug release, J. Control. Release 95 (2004) 391–402.
[19] G. Huang, J. Gao, Z.B. Hu, J.V.S. John, B.C. Ponder, D. Moro, Controlled drug release from hydrogel nanoparticle networks, J. Control. Release 94 (2004) 303–311.
[20] S. Itagaki, M. Sugawara, M. Kobayashi, K. Miyazaki, K. Iseki, Mechanism of active secretion of phenolsulfonphthalein in the liver via Mrp2 (abcc2), an organic anion transporter, Drug Metab. Pharmacokinet. 18 (2003) 238–244.
[21] K. Nishida, N. Sato, H. Sasaki, J. Nakamura, Absorption of organic anions as model drugs following application to rat liver surface in-vivo, J. Pharm. Pharmacol. 46 (1994) 867–870.
[22] Y. Yilmaz, Fluorescence study on the phase transition of hydrogen-bonding gels, Phys. Rev. E: Stat., Nonlinear, Soft Matter Phys. 66 (2002) 052801.
[23] F. Caruso, E. Donath, H. Mohwald, R. Georgieva, Fluorescence studies of the binding of anionic derivatives of pyrene and fluorescein to cationic polyelectrolytes in aqueous solution, Macromolecules 31 (1998) 7365–7377.
[24] S.R. Veith, E. Hughes, S.E. Pratsinis, Restricted diffusion and release of aroma molecules from sol-gel-made porous silica particles, J. Control. Release 99 (2004) 315–327.
[25] J. Siepmann, F. Lecomte, R. Bodmeier, Diffusion-controlled drug delivery systems: calculation of the required composition to achieve desired release profiles, J. Control. Release 60 (1999) 379–389.

[26] K. Shingyouchi, A. Makishima, S. Konishi, Determination of diffusion coefficients of dopants in wet gels during leaching, J. Am. Ceram. Soc. 71 (1988) C82–C84.
[27] K.I. Momot, P.W. Kuchel, Pulsed field gradient nuclear magnetic resonance as a tool for studying drug delivery systems, Concepts Magn. Reson., A 19A (2003) 51–64.
[28] M. Suenaga, Facio: new computational chemistry environment for PC GAMESS, J. Comput. Chem., Jpn. 4 (2005) 25–32.
[29] J.W. Ponder, F.M. Richards, An efficient Newton-like method for molecular mechanics energy minimization of large molecules, J. Comput. Chem. 8 (1987) 1016–1024.
[30] W. Humphrey, A. Dalke, K. Schulten, VMD: visual molecular dynamics, J. Mol. Graph. 14 (1996) 33–38.
[31] J. Crank, G.S. Park, Diffusion in Polymers, Academic Press, New York, 1968.
[32] N. Vahdat, V.D. Sullivan, Estimation of permeation rate of chemicals through elastometric materials, J. Appl. Polym. Sci. 79 (2001) 1265–1272.
[33] J. Siepmann, A. Ainaoui, J.M. Vergnaud, R. Bodmeier, Calculation of the dimensions of drug-polymer devices based on diffusion parameters, J. Pharm. Sci. 87 (1998) 827–832.
[34] J. Park, B. Kahng, R.D. Kamm, W. Hwang, Atomistic simulation approach to a continuum description of self-assembled β-sheet filaments, Biophys. J. 90 (2006) 2510–2524.
[35] F.A. Chmilenko, M.V. Kharun, T.S. Chmilenko, L.V. Sobol', R.B. Gladyshev, Triphenylmethane dye of sulfophthalein series adducts with polyvinylpyrrolidone and their use in chemical analysis, J. Anal. Chem. 56 (2001) 425–428.
[36] C. Rottman, G. Grader, Y. De Hazan, S. Melchior, D. Avnir, Surfactant-induced modification of dopants reactivity in sol-gel matrixes, J. Am. Chem. Soc. 121 (1999) 8533–8543.
[37] Y. Avnir, Y. Barenholz, pH determination by pyranine: medium-related artifacts and their correction, Anal. Biochem. 347 (2005) 34–41.
[38] T. Oya, T. Enoki, A.Y. Grosberg, S. Masamune, T. Sakiyama, Y. Takeoka, K. Tanaka, G. Wang, Y. Yilmaz, M.S. Feld, R. Dasari, T. Tanaka, Reversible molecular adsorption based on multiple-point interaction by shrinkable gels, Science 286 (1999) 1543–1545.
[39] H.J. Chial, H.B. Thompson, A.G. Splittgerber, A spectral study of the charge forms of Coomassie blue G, Anal. Biochem. 209 (1993) 258–266.
[40] W.J. Yong, L.A. Ke, T.Y. Shen, The interaction of bromophenol blue with proteins in acidic solution, Talanta 43 (1996) 1–10.
[41] W.G. Cao, Q.C. Jiao, Y. Fu, L. Chen, Q. Liu, Mechanism of the interaction between bromophenol blue and bovine serum albumin, Spectrosc. Lett. 36 (2003) 197–209.
[42] R. Flores, A rapid and reproducible assay for quantitative estimation of proteins using bromophenol blue, Anal. Biochem. 88 (1978) 605–611.
[43] K.H. Schosinsky, M. Vargas, A. Luz Esquivel, M.A. Chavarria, Simple spectrophotometric determination of urinary albumin by dye-binding with use of bromphenol blue, Clin. Chem. 33 (1987) 223–226.
[44] M.M. Bradford, A rapid and sensitive method for the quantitation of microgram quantities of protein utilizing the principle of protein-dye binding, Anal. Biochem. 72 (1976) 248–254.
[45] S.J. Compton, C.G. Jones, Mechanism of dye response and interference in the Bradford protein assay, Anal. Biochem. 151 (1985) 369–374.
[46] Y.Y. Liu, X.D. Fan, Synthesis, properties and controlled release behaviors of hydrogel networks using cyclodextrin as pendant groups, Biomaterials 26 (2005) 6367–6374.